Aerodynamic Effects of Lift-Jet and Lift-Fan Inlets in Transition Flight

WILLIAM E. GRAHAME*
Northrop Corporation, Norair Division, Hawthorne, Calif.

An investigation was conducted to determine the force and moment contribution of V/STOL lift-jet and lift-fan inlets in transition based on momentum theory. A lift-jet or lift-fan inlet with its axis perpendicular to the freestream develops strong forces that contribute to positive pitching moments at low forward speeds. The analysis is based on the addition of freestream flow with the static-induced flow at the inlet, which is represented by a sink flow over a hemispherical control surface. The results of the analysis, which provide total inlet force, inlet lift, and drag force, as well as inlet lip force and inlet pitching moment, agree reasonably well with a limited amount of published inlet test data. It is shown that the lift-fan inlet develops significantly greater lift, drag, and moment than the lift-jet inlet at comparable thrust and forward speed. Other comparisons are presented which show the close agreement between inlet drag and total incremental jet-induced drag developed by lift fan-in-fuselage and lift fan-in-wing configurations in transition flight.

Nomenclature

A_i = inlet area in plane of inlet
D = drag
D_I = inlet momentum drag
ΔD = interference drag increment due to freestream velocity
d_I = inlet diameter
F = force
L = lift
L_I = inlet momentum lift
ΔL = interference lift increment due to freestream velocity
m = mass flow
M = moment
M_I = inlet moment of momentum
ΔM = interference moment increment due to freestream velocity
p = pressure
r = inlet duct radius
T = thrust
V = velocity
v = static inlet velocity
$\bar{y}$ = moment arm of resultant inlet lift
β = angle of resultant lip force measured from horizontal
θ = coordinate angle
ϕ = coordinate angle
ρ = air density

Subscripts

AERO = aircraft (jet or fan off, inlets closed)
Duct = flow area at inlet plane
I, i = inlet plane
J = jet exit conditions
0 = freestream
R = resultant
S = static conditions
V = forward speed conditions
Lip = inlet lip
TOT = total measured

Introduction

RECENT experience gained from force and moment analyses of lift-jet V/STOL aircraft in transition has indicated several areas that require theoretical treatment. One area, that of the effect of inlet-momentum forces on aircraft in transition, is analyzed here. Other important effects such as the interference forces developed on the wing, body, and tail surfaces because of jet-induced flow still need to be treated. Illustrations of the interference forces developed by typical lift-jet and lift-fan aircraft configurations in transition are shown in Figs. 1a and 1b. In each case, the pattern of the over-all induced flowfield is similar, but the respective forces developed on each configuration vary in magnitude. Such forces result from upwash, downwash, and suckdown, and all are influenced strongly by the proximity of inlets and exits to wing, body, and tail surfaces. With regard to inlet effects, the forces developed are proportional to inlet mass flow, which is higher for the lift fan than the lift jet, and therefore lift-fan inlet forces are higher than lift-jet inlet forces at comparable thrust, as will be shown later.

During transition, the inlet of a lift-jet or lift-fan engine with its axis perpendicular to freestream experiences a large change in force characteristics, primarily because of the inter-

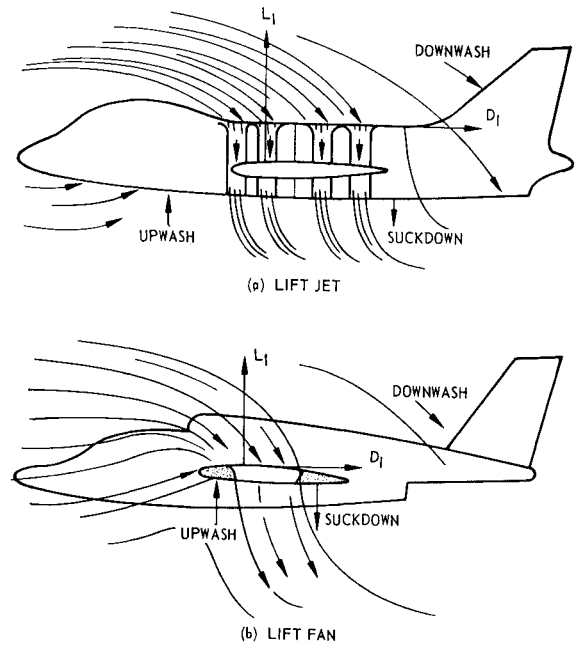

Fig. 1 Lift-jet and lift-fan interference forces in transition.

Presented as Paper 68-637 at the AIAA 4th Propulsion Joint Specialist Conference, Cleveland, Ohio, June 10–14, 1968; submitted June 6, 1968; revision received October 21, 1968.

* Senior Technical Specialist. Member AIAA.

action of the freestream velocity with the induced velocity at the inlet. The force developed at the inlet acts ahead of the inlet axis and is inclined in a rearward direction as a result of the turning of the flow streamtube into the inlet. Thus, a positive moment that is characteristic of similar inflow systems, such as the ducted fan, is created at the inlet.

What is necessary, therefore, is to develop an engineering method applicable to both lift-jet and lift-fan V/STOL aircraft which provides: 1) total inlet forces including inlet lift and drag, 2) inlet lip force, and 3) inlet moment characteristics.

Once these forces and moments are determined, they may be combined with force and moment data of configurations for which exit and other interference effects are available either through method or test. It is assumed in the analysis that the inlet is of optimum shape and separation does not occur. Inlet losses are neglected. Test results described in Refs. 1 and 2 show that inlet inflow distortion of plain inlets in transition is improved considerably with such devices as curved inlet vanes and scoop doors. Another method that has been applied successfully in preventing leading lip separation is that of boundary-layer bleed as described in Ref. 3. Each of the methods is effective in turning the inflow 90° to the freestream.

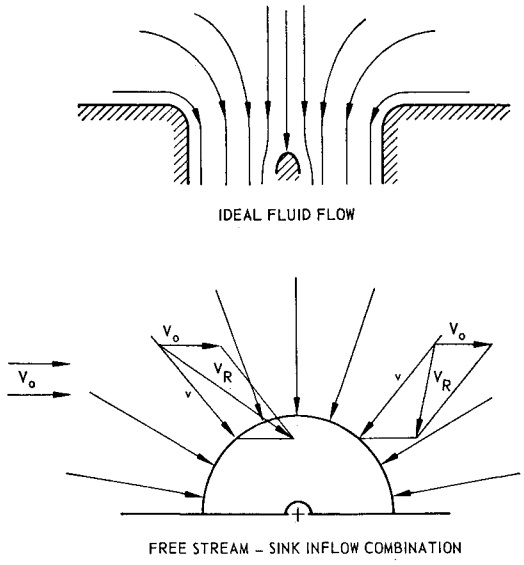

Fig. 3 Inlet-flow representation.

Method Development and Assumptions

Observations of inflow streamline patterns at an inlet of a lift jet or lift fan in transition flight show that the air ahead of the inlet is entrained through angles approaching 90°. This is caused by the viscous shearing action between the inflow produced by the compressor or fan and freestream flow. As a result, a combination of both flows enters the inlet. For a lift jet with a relatively long duct, it may be assumed that the combined inflow velocity is turned completely and is aligned with the axis of the inlet (Fig. 2a). In the case of a lift fan with a relatively thin duct, as in a wing (Fig. 2b), it may be assumed that the combined inflow is not turned axially, but at an angle ϕ with the horizontal, as shown in Fig. 2b. This is particularly true at the higher forward speeds, where the angle ϕ decreases. In the analysis which has been conducted, the inflow at forward speeds is assumed to be turned axially ($\phi = 90°$) at the inlet plane. This is an approximation since there is uncertainty concerning actual inflow angles. As will be shown later, it is deduced that this assumption apparently is valid except at high transition speeds where crossflow angles are high (see discussion of Fig. 15). At such speeds and low fan-induced velocities (low angle of ϕ), the inflow will separate below the forward inlet lip as shown typically in Fig. 2b. Experimental tests of lift-engine inlets have been conducted by Tyson[1] and Lavi,[2] both of whom show inlet conditions responsible for inlet flow separation. Total pressure loss and inlet flow-distortion characteristics at several freestream to inlet velocity ratios are presented. However, in both cases, force and moment measurements were not included.

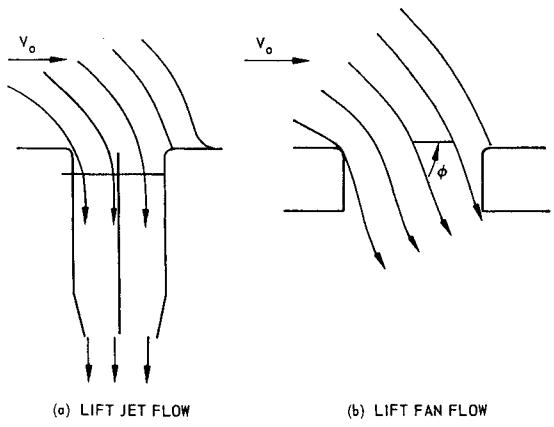

Fig. 2 Inlet- and exit-flow comparison.

At the present time, a limited amount of experimental tests have been made concerning inlet lift, and drag and moments on lift engines. Inlet model tests of lift jets performed by Kuhn and McKinney[4] indicate that inlet drag corresponds exactly to momentum drag. It is suggested in their paper that the pitching moment is equivalent to the inlet drag acting at a distance of a little over one inlet diameter above the upper surface of the body. However, the pitching moment actually results from the lift imbalance fore and aft across the inlet. Ram or momentum drag should act at the inlet plane and not contribute to pitching moment except when the moment center lies below the inlet. At this point, mention should be made concerning the composition of inlet lift. The total inlet lift force is comprised of lift on both the inlet lip and the lift developed over the compressor or fan. The method applies to conditions where the angle of attack and sideslip angle are zero degrees.

Until the present, a negligible amount of work has been applied to determine analytically the force and moment contribution of inlets in transition. As a result of recent experience in the analysis of momentum effects of lift-fan and lift-jet inlets, it is determined that a simplified method that predicts inlet forces and moments is required. It is the purpose of this paper to develop expressions that define inlet lift and its location, as well as drag and pitching moment, for lift-jet and lift-fan applications. This is accomplished by a simplified momentum analysis that considers the vector addition of freestream velocity with that of an ideal sink-flow distribution. The assumption made is that the ideal sink inflow is representative of that for an actual velocity inflow distribution about an inlet at static conditions. This analogy is presented in Fig. 3, which compares an ideal fluid-inflow profile with that of a sink inflow. In the lower part of Fig. 3, freestream velocity V_0 is imposed upon the sink inflow, and the resulting velocity components V_R clearly indicate the disproportionate velocity distribution across an inlet. It is indicated that the origin of separation at the forward inlet lip is due to the resulting high angularity of the forward velocity with respect to the forward wall.

By imposing freestream velocity V_0 upon a sink flow v over a hemispherical control surface as developed by Theodorsen,[5] a three-dimensional velocity field about the inlet is represented, as shown in Fig. 4. The components of velocity are: $V_x = v \sin\phi \cos\theta$, $V_y = v \sin\phi \sin\theta + V_0$, and $V_z = v \cos\phi$. The resultant velocity entering the hemispherical control

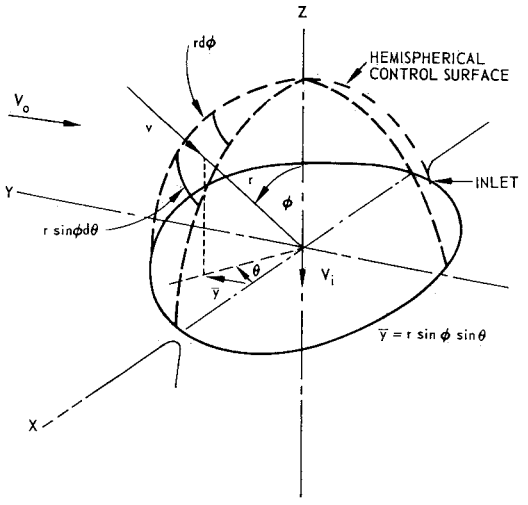

Fig. 4 3-dimensional velocity field.

surface of radius r is then

$$V_R^2 = V_0^2 + 2V_0 v \sin\varphi \sin\theta + v^2$$

An approximation is made in which it is assumed that the resultant velocity V_R is turned axially at the inlet plane. An increase in velocity at the inlet therefore is experienced over that for the static case. A departure from the analysis by Theodorsen is made in Ref. 6 to permit the development of expressions for inlet momentum lift. The inlet is divided into two halves, a front or upstream half and a rear half. Expressions for lift are developed for both portions, where

$$L_{\substack{\text{inlet}\\\text{front}\\\text{half}}} = 2\int_{\phi=0}^{\pi/2}\int_{\theta=0}^{\pi/2} \rho V_R^2 r^2 \sin\varphi \cos\varphi \, d\phi \, d\theta$$

$$= 2\rho\int_{\varphi=0}^{\pi/2}\int_{\varphi=0}^{\pi/2} (V_0^2 + 2V_0 v \sin\varphi \sin\theta + v^2) \times r^2 \sin\varphi \cos\varphi \, d\phi d\theta \tag{1}$$

$$L_{\substack{I\\\text{front}\\\text{half}}} = \frac{\rho A_i}{2}\left[V_0^2 + \frac{8}{3\pi} V_0 v + v^2\right]$$

Similarly, the integral equation of the inlet momentum lift in the rear half of the duct is given by

$$L_{\substack{\text{inlet}\\\text{rear}\\\text{half}}} = 2\rho\int_{\varphi=0}^{\pi/2}\int_{\varphi=-\pi/2}^{0} (V_0^2 + 2V_0 v \sin\varphi \sin\theta + v^2) \times r^2 \sin\varphi \cos\varphi \, d\phi d\theta$$

Then

$$L_{\substack{I\\\text{rear}\\\text{half}}} = \frac{\rho A_i}{2}\left[\left(V_0^2 - \frac{8}{3\pi} V_0 v + v^2\right)\right] \tag{2}$$

Comparison of Eqs. (1) and (2) shows clearly the disproportionate lift distribution across the inlet. This develops as a result of a greater amount of mass in the forward portion compared to that in the rear portion.

Combining Eqs. (1) and (2), the total inlet momentum lift is

$$L_I = \rho A_i (V_0^2 + v^2) \tag{3}$$

where $(V_0^2 + v^2)$ is the square of the integrated velocity that is assumed to act at the inlet plane, and therefore

$$L_I = \rho A_i V_i^2 = m V_i \tag{4}$$

Upon inspection of Eq. (3) it may be noted that inlet lift is composed of $\rho A_i V_0^2$ and $\rho A_i v^2$. The latter term is the static lift developed at the inlet, while the former term is the lift produced as a result of entrainment. Experimental tests are required to verify this portion of the total inlet momentum.

The drag of the inlet due to arrest of inlet momentum is

$$D_I = \rho A_i (V_0^2 + v^2)^{1/2} V_0$$

or

$$D_I = \rho A_i V_i V_0 = m V_0 \tag{5}$$

The moment of the inlet is developed using expressions for lift acting at a moment arm $\bar{y} = r \sin\varphi \sin\theta$. Then,

$$M_{\substack{I\\\text{front}\\\text{half}}} = 2\rho\int_{\varphi=0}^{\pi/2}\int_{\theta=0}^{\pi/2} (V_0^2 + 2V_0 v \sin\varphi \sin\theta + v^2) r^3 \sin^2\varphi \cos\varphi \sin\theta \, d\varphi d\theta \times$$

or

$$M_{\substack{I\\\text{front}\\\text{half}}} = \frac{2}{3}\rho r^3 V_0^2 + \rho\frac{\pi r^3 V_0 v}{4} + \frac{2}{3}\rho r^3 v^2 \tag{6}$$

Similarly, the moment of inlet lift in the rear half is

$$M_{\substack{I\\\text{rear}\\\text{half}}} = 2\rho\int_{\varphi=0}^{\pi/2}\int_{\theta=-\pi/2}^{0} (V_0^2 + 2V_0 v \sin\varphi \sin\theta + v^2) \times r^3 \sin^2\varphi \cos\varphi \sin\theta \, d\varphi d\theta$$

or

$$M_{\substack{I\\\text{rear}\\\text{half}}} = -\frac{2}{3}\rho r^3 V_0^2 + \rho\frac{\pi r^3 V_0 v}{4} - \frac{2}{3}\rho r^3 v^2 \tag{7}$$

Thus, it is shown on the basis of Eqs. (6) and (7) that moment contribution of the forward portion is greater than the rear portion, which results in a positive moment. Again, by combining Eqs. (6) and (7), the total moment developed at the inlet is

$$M_I = \rho(\pi r^3 V_0 v/2) \tag{8}$$

The moment arm about the X axis is defined as

$$\bar{y} = M_I/L_I = r^3 V_0 v/2r^2(V_0^2 + v^2) \tag{9}$$

or

$$\bar{y} = (r/2)(V_0 v/V_i^2) \tag{10}$$

Equation (10) shows that the moment arm varies as the velocity ratio $V_0 v/V_i^2$.

The preceding inlet force and moment characteristics essentially represent the forces and moments that result from the change in direction of the mass flow within the inflow streamtube. This is shown schematically in Fig. 5.

Inlet Lip Forces

It is now of interest to establish on the basis of the total inlet force that portion which acts on the lip as opposed to the force developed across the inlet area A_i of the duct.

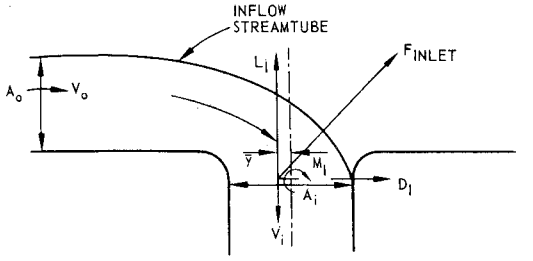

Fig. 5 Inlet force and moment characteristics.

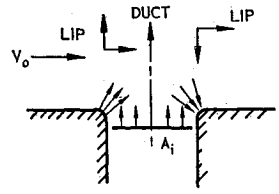

Fig. 6 Inlet lip and duct forces.

Figure 6 shows a simplified breakdown of these forces. Therefore, $L_I = L_{Lip} + L_{Duct}$.

L_{Duct} is the lift produced by the compressor or fan and is obtained by multiplying the inlet area A_i by the difference in static pressure $(p_i - p_0)$. A further development of the duct lift is shown later. The lift on the lip can be shown as

$$L_{Lip} = mV_i + (p_i - p_0)A_i \tag{11}$$

The drag due to the inlet lip is equivalent to inlet or ram drag in Eq. (5) and is therefore

$$D_{Lip} = mV_0$$

These expressions can be combined according to the vector sketch in Fig. 7 to obtain F_{Lip}. Therefore,

$$F_{Lip} = \{(mV_0)^2 + [mV_i + (p_i - p_0)A_i]^2\}^{1/2}$$

This analysis has been shown previously by Tyson[1] and is representative of an inlet with its axis perpendicular to the freestream.

For incompressible flow

$$(p_i - p_0) = \tfrac{1}{2}\rho V_0^2 - \tfrac{1}{2}\rho V_i^2$$

Then,

$$F_{Lip} = [(mV_0)^2 + (\tfrac{1}{2}mV_i + \tfrac{1}{2}\rho A_i V_0^2)^2]^{1/2} \tag{12}$$

A relation can then be developed which shows the ratio of F_{Lip} to inlet lift L_I according to Eqs. (12) and (4) as shown in Fig. 8;

$$\frac{F_{Lip}}{L_I} = \frac{[(V_0/V_i)^4 + 6(V_0/V_i)^2 + 1]^{1/2}}{2} \tag{13}$$

The lip lift can be expressed as

$$L_{Lip} = mV_i + \tfrac{1}{2}\rho A_i(V_0^2 - V_i^2) \tag{14}$$

The relationship L_{Lip}/L_I shown in Fig. 8 is derived from preceding Eqs. (14) and (4) where

$$L_{Lip}/L_I = \tfrac{1}{2}[1 + (V_0/V_i)^2] \tag{15}$$

The force developed across the inflow duct area A_i is the duct lift, which can be shown as

$$L_{Duct} = \tfrac{1}{2}\rho A_i(V_i^2 - V_0^2)$$

Since $V_i^2 = V_0^2 + v^2$ from Eq. (3),

$$L_{Duct} = \tfrac{1}{2}\rho A_i v^2 \tag{16}$$

Thus, the duct lift remains constant at the static value at forward speed conditions.

Returning to the inlet lip, the lip lift can be expressed as

$$L_{Lip} = \rho A_i V_0^2 + \tfrac{1}{2}\rho A_i v^2 \tag{17}$$

In consideration, then, of the results in Eqs. (16) and (17), it is evident that of the total inlet lift L_I, $\rho A_i V_0^2$ is the amount of lift developed above the level of static lift at forward speed. The lift increment $\rho A_i V_0^2$ is due to entrainment, and occurs

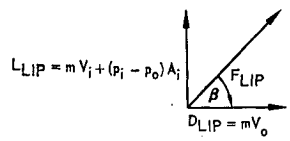

Fig. 7 Inlet lip force relations.

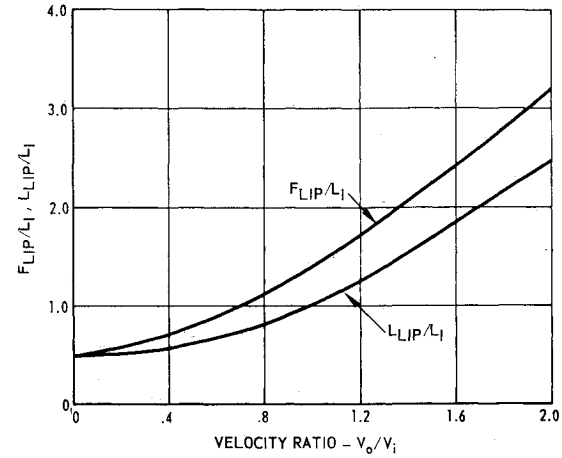

Fig. 8 Inlet force vs velocity ratio.

on the inlet lip. These conclusions are in agreement with results in Ref. 7.

Application of Method

It is of interest now to apply the results to a representative lift jet and lift fan that produce a static thrust of 3000 lb. The lift, drag, and moment of a lift jet with inlet and exit areas of 1.4 ft² and 0.76 ft², respectively, and a lift fan of constant area = 20 ft² are compared in Fig. 9 based on the previous equations for lift (4) and (15), drag (5), and moment (8). It is seen in each case that the contribution of the lift-fan inlet is significantly greater than that of the lift-jet inlet. This is because of the much greater momentum that enters the lift-fan inlet during transition. It should be pointed out that the inlet lift L_I, developed by the lift jet, is only that portion which is developed at the inlet plane. For the example shown in Fig. 9, this amounts to an average of 20% of the static thrust. For the lift fan, assuming a constant-area duct,

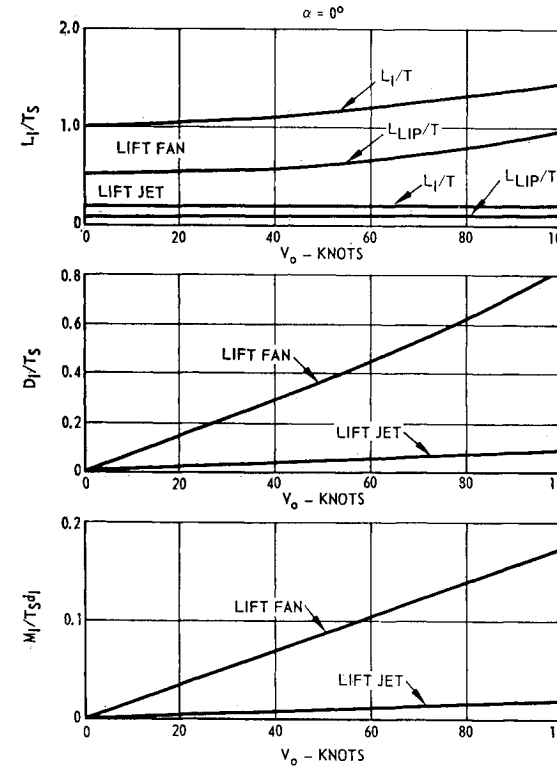

Fig. 9 Inlet force and moment: lift-fan, lift-jet comparison.

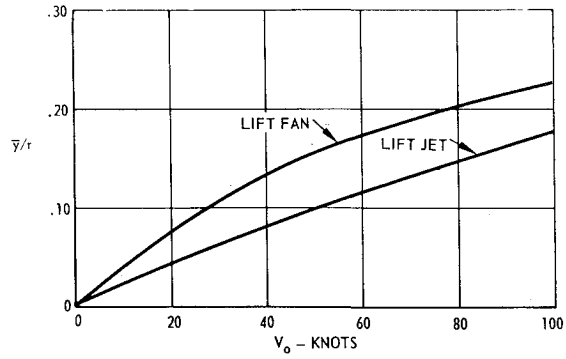

Fig. 10 Moment-arm comparison.

inlet lift is equivalent to the static thrust produced at zero speed, and increases faster with increasing speed than the lift jet. Lift-fan inlet drag is seen to be approximately 8 times that of the lift-jet inlet at 100 knots. At this speed, the moment of the lift-fan inlet is approximately 10 times that of the lift jet. This, again, is due to the greater momentum of the lift fan acting about a larger moment arm. A comparison of the moment arm for the example lift jet and lift fan was obtained from (10) and is presented in Fig. 10.

Experimental Data Comparisons

With the exception of test results of lift-jet configurations of Refs. 4 and 8, there appear to be very little inlet force and moment data available for direct comparison with the methods developed. Even the inlet test data from these two references include interference forces on adjacent surfaces. However, it was considered of interest to show relative comparisons of these data with that of the inlet method.

Experimental incremental force and moment inlet characteristics are computed on the basis of the following parameters at an angle of attack of zero degrees for forward speed

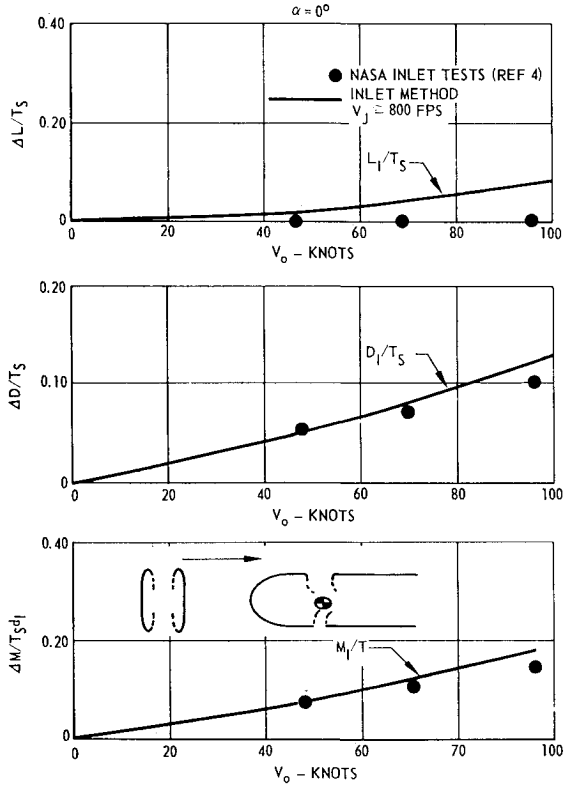

Fig. 11 Lift-jet inlet lift, drag, and moment.

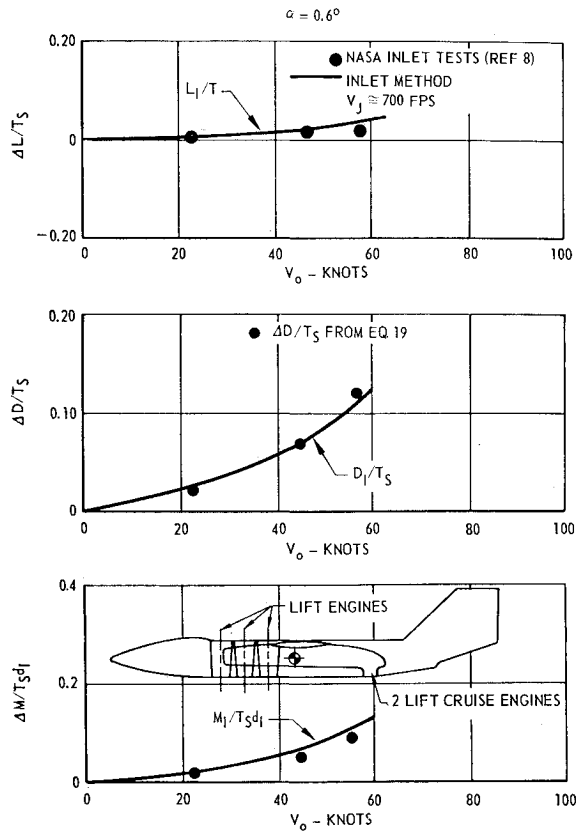

Fig. 12 Multiple jet in fuselage.

conditions where

$$\Delta L/T_S = L_{TOT}/T_S - (T_S + L_{AERO})/T_S \quad (18)$$

$$\Delta D/T_S = (D_{TOT} - D_{AERO})/T_S \quad (19)$$

$$\Delta M/T_S d_I = (M_{TOT} - M_{AERO})/T_S d_I \quad (20)$$

The experimental inlet test data increments include induced upwash and downwash and inlet momentum effects.

Figure 11 from Ref. 4 presents inlet data for the simulation of a single engine in a body. The model was set up so that the air drawn into the inlet was pumped off independently of the exit. The test results show zero lift increment with forward speed, since mass flow was maintained constant. The lift increase shown for the inlet method includes the effects of increased mass flow with forward speed. Reference 8 provides simulated lift-jet data for a five-jet test model con-

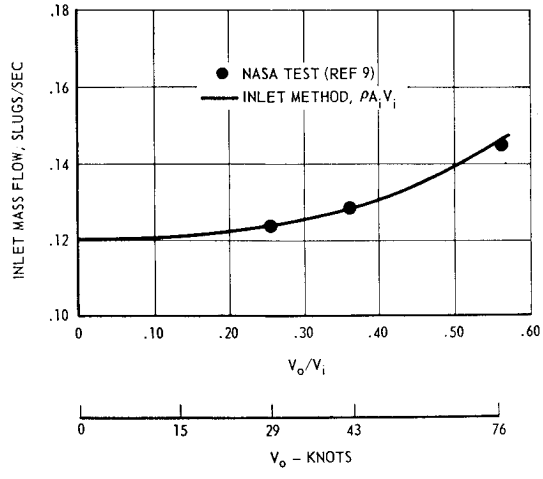

Fig. 13 Effect of airspeed on fan performance.

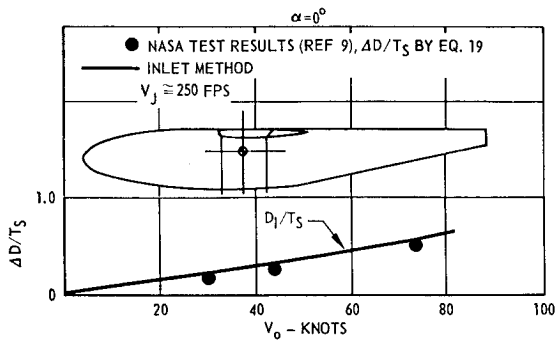

Fig. 14 Lift fan in fuselage.

figuration. The incremental lift and moment test data from Ref. 8 as shown in Fig. 12 reflect the difference of open and closed inlets. The drag increments shown in Fig. 12 were calculated according to Eq. (19), since comparative inlet drag data in Ref. 8 were not shown. The apparent good agreement between the drag data points $\Delta D/T$ and the inlet-method curve D_I/T indicates that the method is a useful tool for predicting total drag increments due to the effects of power. This is in consideration of the fact that induced effects other than that directly at the inlet contribute a negligible amount to drag.

The comparison shown in Fig. 13 shows most effectively that inlet mass flow at forward speed can be predicted by the inlet method where mass flow is equivalent to $\rho A_i(V_0^2 + v^2)^{1/2}$. The test data were obtained from Ref. 9, which shows tests of a small-scale, 7-in., fan-in-fuselage model at forward speed, as shown in Fig. 14. The drag comparison presented in Fig. 14 again indicates close agreement between $\Delta D/T$ and D_I/T.

Since there appeared to be good agreement between the inlet drag method and test, it was decided to extend the comparison to the aerodynamic data of Refs. 10 and 11, for which data were available. The lift-fan configurations illustrated in Figs. 15 and 16 were equipped with the same fan with a diameter of 62.5 in., and were powered by J-85 gas generators.

Test data for the full-scale fan-in-wing configuration in Fig. 15 compare quite closely to the inlet method. A possible indication of inlet flow separation may be noted in Fig. 15 at a speed of approximately 72 knots, where drag data bend away from the trend established by the inlet method. Figure 16 presents a comparison of drag data for a full-scale XV-5A configuration. The data fall below the inlet method curve for most of the speed range, possibly indicating that inlet flow is not completely turned in the axial direction.

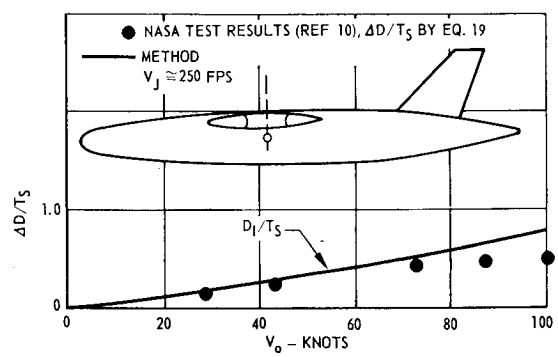

Fig. 15 Lift fan in wing.

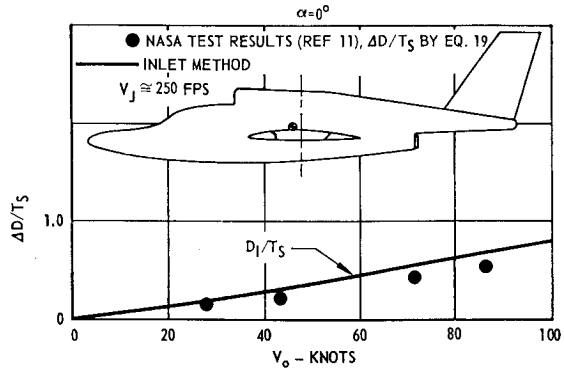

Fig. 16 XV-5A lift-fan data.

Conclusions

In consideration of the objective of this investigation, the following conclusions are stated: 1) a method for determining total inlet momentum lift, inlet lip lift, and inlet moment of lift-jet and lift-fan configurations in transition flight has been developed; 2) the location of both inlet momentum lift and drag with respect to the duct centerline has been established; 3) the results presented show reasonably good agreement between D_I/T_S and $\Delta D/T_S$, indicating that the inlet method appears to be useful in predicting total incremental drag at forward speed. Since there is a lack of directly applicable inlet test data, it is recommended that experimental tests be conducted to verify the methods presented.

References

[1] Tyson, B. I., "Tests to Establish Flow Distortion Criteria for Lift Engines," *Journal of Aircraft*, Vol. 2, No. 5, Sept.-Oct. 1965, pp. 411–417.

[2] Lavi, R., "An Experimental Investigation of VTOL Jet-Engine Inlet," *Journal of Aircraft*, Vol. 4, No. 2, March-April 1967, pp. 125–132.

[3] Schaub, U. W., "Experimental Studies of VTOL Fan-in-Wing Inlets," Agardograph 103, Pt. II, Oct. 1965, NATO.

[4] Kuhn, R. E. and McKinney, M. O., "NASA Research on the Aerodynamics of Jet VTOL Engine Installations," Paper, Oct. 1965, AGARD.

[5] Theodorsen, T., "Theoretical Investigation of Ducted Propeller Aerodynamics," TRECOM Report, Vol. I, CRD 3860, Aug. 1960, U. S. Army.

[6] Grahame, W. E., "An Experimental and Analytical Investigation of a Ducted Fan in a Lifting Surface Including the Effects of a Flap," Appendix, Master's thesis, 1964, Univ. of Colorado.

[7] Hackett, J. E., "Wind Tunnel Tests on a Streamlined Fan Lift Nacelle," Pt. II, R&M 3470, Oct. 1965, British Aeronautical Research Council.

[8] Margason, R. J. and Gentry, G. L., "Aerodynamic Characteristics of a Five-Jet VTOL Configuration in the Transition Speed Range," Working Paper 325, Nov. 16, 1966, Langley Research Center.

[9] Davenport, E. E. and Kuhn, R. E., "Wind Tunnel Wall Effects and Scale Effects on a VTOL Configuration with a Fan Mounted in a Fuselage," TN D-2560, Jan. 1965, NASA.

[10] Hickey, D. H. and Hall, L. P., "Aerodynamic Characteristics of a Large-Scale Model with Two High Disk-Loading Fans Mounted in the Wing," TN D-1650, Feb. 1963, NASA.

[11] Kirk, J. V., Hickey, D. H., and Hall, L. P., "Aerodynamic Characteristics of a Full-Scale Fan-in-Wing Model Including Results in Ground Effect with Nose-Fan Pitch Control," TN D-2368, July 1964, NASA.